Single-Particle Diffusion into a Disordered Matrix: Simulation of a Metal–Polymer Interface

B. D. Silverman

IBM Research Division, T. J. Watson Research Center, Yorktown Heights, New York 10598

Received August 3, 1990; Revised Manuscript Received November 6, 1990

ABSTRACT: A sensitive radiotracer technique has recently been utilized to examine the diffusion of copper atoms from the surface into the bulk of thin copper-deposited polyimide films upon annealing. Characteristics of the metal atom concentration profile were discussed in connection with Monte Carlo simulation studies. The present paper describes the simulation model in some detail and focuses upon the formation of metal atom clusters in the region near the film surface. Qualitative aspects of the copper atom diffusion will be shown to be consistent with the results of the Monte Carlo study. Furthermore, the dependence of metal atom cluster shape and distribution upon the interaction between the metal atoms will be examined.

I. Introduction

The copper–polyimide interface has attracted wide attention[1-7] due to its potential for utilization in microelectronic circuitry. While one would surmise that the electrical characteristics of a copper–polyimide interface should appear optimal, the actual synthesis of such interface, exhibiting desired mechanical and chemical properties, has been elusive.

The relatively weak binding between copper atoms and the polyimide yields interfaces characterized by poor adhesion and uniformity with interfacial regions of significant extent that are composed of copper aggregates imbedded in the polymeric matrix.[3,6] Fundamental studies of such interesting two-phase interfacial regions have proceeded in an attempt to yield insight concerning successful strategies for synthesizing interfaces of technological significance.

Monte Carlo simulations have been previously performed to assist with the interpretation of transmission electron micrographs[6] and radiotracer diffusion studies[7] of the copper–polyimide interface. In the present paper the model that such studies were based upon will be described and results appropriate for interpretation of the radiotracer studies will be examined in greater detail than heretofore. Such simulations enable one to predict the qualitative changes expected upon varying the conditions under which the metal–polymer interface is created and provide one with deeper insight into the origin of such changes.

II. Model

a. Simulated Polymer. The calculations are performed on a three-dimensional grid that is 81 × 81 × 51 lattice spacings in extent. Grid indices run from −40 to 40 along the longer dimensions and from -30 to 20 along the short dimension. The direction perpendicular to the plane of the film is along the short dimension. Ten units along this dimension, k = -30 to -21, are reserved for the vacuum above the film in the absence of film metalization. This will allow metalized islands to form above the film surface and also provide for the capability of investigating the formation of continuous films at higher metal depositions than treated in the present paper.

The polymer is idealized by a set of "interaction sites". These polymer interaction sites are designated by a set of occupied grid positions. The designation "polymer interaction site" is used since it is assumed that metal atoms will bind when at grid positions that are nearest neighbors to these sites. Consistent with the density of interaction sites that are chosen, crude arguments concerning polyimide structures and the various functional groups of the polymer that might interact with a metal atom suggest that the grid point separation of our lattice is of the order of several angstroms. Since the metal atoms are also confined to the grid positions, the density of interaction sites chosen on the fixed grid also determines the "openess" of the structure or the ease with which a metal atom may perform a random walk through the polymeric matrix. For the present calculations we have initially chosen the interaction sites to be distributed in a regular array, over every third grid position from -39 to 39 along the lateral box dimensions and from -19 to 19 over the film thickness dimension. Therefore, 10 206 such sites are distributed initially in this manner over the three-dimensional grid and this number is conserved in all the calculations that we will describe.

The interaction sites perform their own random walk via single jumps to nearest-neighbor grid positions. These sites are, however, constrained to move within the vertical dimension, from a grid position with k = -20 to k = 20. The sites are, therefore, not allowed to move into the "vacuum", i.e., onto grid positions with k = -30 to k = -21. The interaction site positions are randomized by a Monte Carlo calculation prior to metal atom deposition. Even though there is no ordered distribution of such sites in the vicinity of k = -20 after the Monte Carlo randomization, the set of grid positions with k = -20 can be thought of as the "surface" of the film. This is so, since the algorithm that we will choose to simulate metal atom deposition through flash evaporation treats metal atoms that are above the film, i.e., at grid positions above the surface of the film (k = -30 to -22), differently from metal atoms that are either adjacent to the film surface (k = -21) or inside the film (k > -21). The Monte Carlo thermalization of the interaction site distribution, prior to metalization, is terminated after the averages of certain spatial correlation functions indicate that the interaction site distribution has achieved steady state.

Figure 1a shows a three-dimensional view of the interaction site distribution after thermalization and prior to metal deposition. The line of sight is at an angle with respect to the top surface. Figure 1b shows the two-dimensional site distribution in a slice of the film (at one particular value of index) along one of the two lateral directions. The distribution or degree of order of the polymer interaction sites is determined by the interaction energies between the sites. At present, we have assumed

0024-9297/91/2224-2467$02.50/0

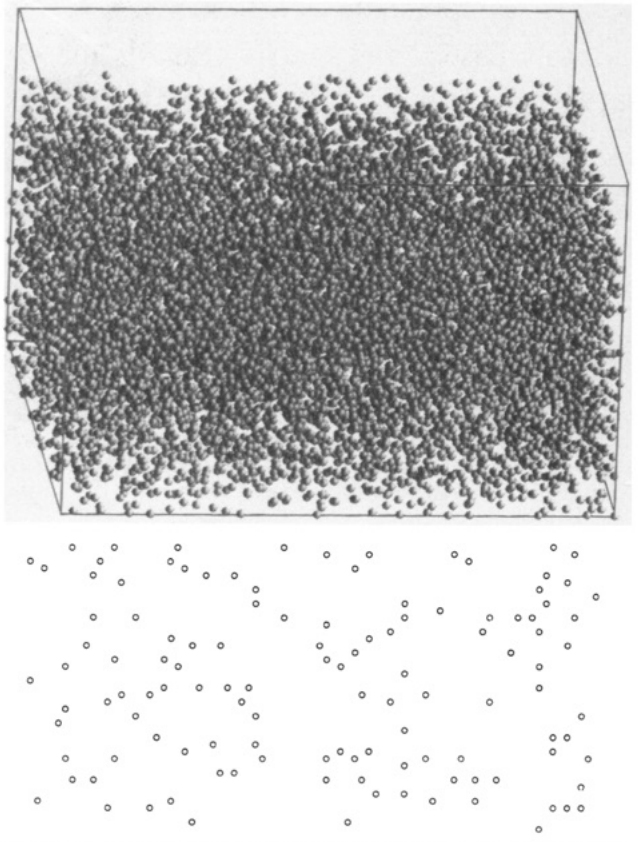

Figure 1. Polymer interaction site distribution. (a, Top) Three-dimensional view at an angle to the top "surface" prior to metal atom deposition. (b, Bottom) Interaction site distribution in a plane perpendicular to one of the lateral directions.

only a nearest-neighbor and next-nearest-neighbor repulsion between the interaction sites. Distances between nearest neighbors and next nearest neighbors are 1 and $\sqrt{2}$ lattice parameters, respectively. The values of the repulsive energies that have been chosen, namely, 0.2 eV, considerably exclude occupancy of such grid positions at the temperature for which all calculations will be performed, namely, 320 °C. On the other hand, the relatively low initial interaction site density that we have chosen does provide for significant motion of the interaction sites during thermalization. Sites are able to easily migrate between grid positions that are not either nearest or next nearest neighbors to any other interaction site. Instead of starting from an ordered interaction site density, one might have performed the Monte Carlo thermalization of the initial interaction site distribution from a set of 10 206 randomly distributed sites.

Periodic boundary conditions are imposed for the two lateral directions in the plane of the film. Furthermore, the film is assumed to be on an impenetrable substrate, the film grid index along the short dimension adjacent to this substrate is given by $k = 20$. Neither polymer interaction sites nor metal atoms are allowed to jump into the substrate.

b. Simulated Metal Atom Deposition. One-quarter monolayer metalization is achieved by randomly selecting two grid indices that define a trajectory normal to the film surface. The metal atom is then moved into the film, from negative k values, and brought to rest at a grid position in the film when for $k < -21$ it encounters a metal atom in front of it and for $k > -22$ (a) it encounters a polymer interaction site as a nearest neighbor or (b) it encounters a nearest neighbor or next nearest neighbor grid position occupied by a metal atom.

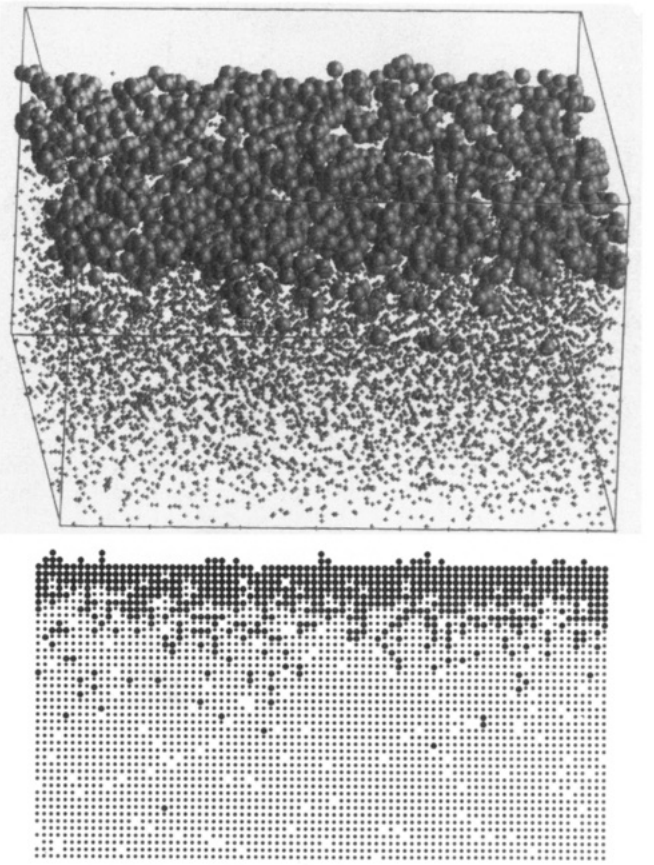

Figure 2. (a, Top) Three-dimensional view, at an angle to the top film surface, after deposition of one-quarter monolayer of metal atoms. The metal atoms are shown as larger spheres. (b, Bottom) Metal atom penetration profile into the film just after initial metalization.

By choosing the rule of deposition in this fashion we have implicitly imposed what has been called an "SOS restriction" above the film surface so that overhanging structures are excluded.[8] The deposited metal atoms do, therefore, sense a "film surface", at k = -20, even though they may be deposited in a local region devoid of polymer interaction sites.

Such details associated with the deposition process are of little consequence for the present simulation due to the small number of metal atoms deposited. They will be of significance, however, when details associated with the formation of continuous films are investigated.

The initial metalization, which simulates the flash evaporation,[7] is terminated after 1640 metal atoms have been so deposited; essentially one-quarter of a monolayer. Figure 2a shows a three-dimensional view, at an angle to the top surface, of the distribution of metal atoms. Figure 2b shows an edge-on view of the film just after this metalization step. Due to the partially random distribution of interaction sites at relatively low density, initial metalization yields a metal atom penetration profile into the polymer, shown in Figure 2b, that is not insignificant. In generating Figure 2b, we have assumed that one sees a metal atom if there is one anywhere along the line of sight edge-on to the film. If not, then one sees a polymer interaction site, if there is at least one along the line of sight. An empty grid position indicates that along the line of sight there is neither a metal atom nor polymer interaction site through the entire film thickness.

c. Simulated Annealing and Diffusion. It is assumed that metal atom migration occurs as a result of

only single metal atom jumps to empty nearest-neighbor grid positions. Migration of any cluster that is formed is therefore a consequence of a series of single metal atom jumps. One expects this assumption to preclude a realistic simulation of the large metal atom clusters observed in the TEM[6] at higher coverages. It should, however, yield a reasonable representation of the initial stages of cluster formation resulting mainly from single particle agglomeration.

The calculation is performed as follows: First, the Monte Carlo calculation is performed over the set of polymer interaction sites such that each site is addressed on average two times before the metal atom distribution is addressed. The distribution of interaction sites is therefore allowed to relax in the presence of the metal atoms. This feature has been introduced into the model since the TEM results[6] suggest that, upon annealing, polymer material is extruded during the formation of the observed metal globules.

Prior to metalization, the interaction sites had been thermalized at the temperature of the anneal, 320 °C. Systematic changes in the interaction site distribution statistics upon metalization should, therefore, reflect interaction site relaxation in the presence of the metal atom distribution. Each metal atom is addressed, on average, 100 times during the metal atom Monte Carlo step. The division between numbers of interaction site and metal atom grid position addresses is at present arbitrary but chosen with the thought that the polymer relaxation is a significantly slower process than the metal atom relaxation. Slow polymer relaxation with respect to the motion of small molecular penetrants is a complicating feature of the diffusion of such penetrants into polymers below the glass transition temperature.[9] After the metal atom Monte Carlo step, the calculation then loops back to the beginning of the interaction site Monte Carlo step. The total number of times that the "interaction site–metal atom" Monte Carlo sequence is performed corresponds to the amount of elapsed time one wishes to simulate. The Metropolis procedure is used throughout.[10]

A qualitative time scale with respect to experimental annealing times is determined as follows: The Arrhenius plot, Figure 2 of ref 7, had been obtained in the Fickian regime of diffusion. One might therefore expect the activation energy associated with the three high-temperature points of this plot to yield a measure of the binding energy of single copper atoms to the polymer interaction sites. The activation energy obtained from these three points is approximately equal to 0.2 eV. In the present calculations we have chosen the binding energy of a copper atom to a nearest-neighbor polymer interaction site to be 0.1 eV. This smaller value is chosen since the simulation model involves a significant number of metal atoms bound to two interaction sites. Furthermore, we expect the smaller value to speed up metal atom diffusion over that experimentally observed and consequently reduce the cpu time required to achieve a quasi-stationary nonequilibrium steady state of the system.

For single particle diffusion with a single activated jump time, the diffusion constant for random walk on an empty 3-d lattice can be written:

$$D = (\nu/6)a^2 \exp(-E/KT) \quad (1)$$

The diffusion constant, D, experimentally obtained[7] for the 320 °C anneal, is approximately 1.0×10^{-14} cm^2/s. As previously mentioned, one expects the lattice parameter, a, to be several angstroms. ν is the average number of times that the metal atom is addressed per second during the Monte Carlo calculation. During the metal atom Monte Carlo calculation, a random number generator chooses a grid position on the lattice to be interrogated. If a metal atom is at this grid position, the Metropolis algorithm[10] is used to determine the metal atom motion. On average, each metal atom will be addressed once during a number of random number generator calls equal to the total number of grid points, namely, $81 \times 81 \times 51$ (334 611). We will define the metal atom Monte Carlo loop with this number of random number generator calls to be "one Monte Carlo cycle" or "the Monte Carlo cycle".[11] Each Monte Carlo cycle is therefore representative of some unit of elapsed time, independent of the number of metal atoms distributed on the grid. With use of eq 1, the value of the diffusion constant and activation energy, and an estimate of the lattice parameter, one can obtain a value for ν, the number of Monte Carlo cycles per second. In this manner we find that approximately 200 cycles correspond to 1 s. Since we have chosen 100 Monte Carlo cycles for the metal atom Monte Carlo loop, then two interaction site–metal atom sequences correspond to approximately 1 s of experimentally elapsed annealing time.

It should be emphasized that eq 1 describes diffusion associated with a much simpler model than we are treating. The simulation model involves more than a single activation energy for metal atom migration. Aside from the number of metal atoms bound to a single polymer interaction site, there are significant numbers of metal atoms bound to no host interaction sites and significant numbers of metal atoms bound to two interaction sites. Also, the calculation involves restricted random walks due to the presence of other metal atoms as well as interaction sites. Equation 1 has, therefore, been used only as a guide in setting up an approximate correspondence between experimental annealing times and the calculated diffusion times of our model simulation.

Table I[a]

MC	M	C0	C1	C2	C3
0	1640	693	927	20	0
200	1594	459	985	150	0
400	1516	306	1032	178	0
600	1465	229	1014	222	0
800	1408	341	852	215	0
1000	1363	261	864	237	1
2000	1220	154	813	253	0
3000	1128	141	765	222	0
4000	1058	129	702	227	0
5000	1007	101	698	208	0

[a] MC, number of Monte Carlo cycles; M, total number of metal atoms; $C0$, number of metal atoms not bound to any polymer interaction site; $C1$, number of metal atoms bound to a single polymer interaction site; $C2$, number of metal atoms bound to two polymer interaction sites; $C3$, number of metal atoms bound to three polymer interaction sites.

III. Simulated Annealing

a. Vanishing Interaction Energy between Metal Atoms. First, we will examine diffusion under the condition that the interaction between the metal atoms is arbitrarily turned off. These calculations have been performed to see if the observed diffusion is in qualitative accord with what is to be expected from the choice of model parameters. Subsequent calculations with the metal atom interaction turned on will yield results with significantly reduced metal atom diffusion.

Table I lists information concerning the binding of the metal atoms to the polymer interaction sites at different time steps of the calculation. The first few time steps are listed in intervals of 200 Monte Carlo cycles. After five

of these steps the time interval has been increased. Listed in the table are MC, the number of Monte Carlo cycles; M, the total number of metal atoms; $C0$, the number of metal atoms not bound to any host site; $C1$, the number of metal atoms bound to a single host interaction site; and so forth.

One sees that the total number of metal atoms is significantly reduced as the calculation proceeds without the the interaction turned on between metal atoms. This occurs due to reemission or desorption of metal atoms from the film surface into the vacuum and their eventual escape from the system. We have assumed that if a metal atom migrates to the top of the grid, i.e., to a position for which $k = -30$, and then makes a jump in the negative k direction, it is lost to the system forever. Further examination of Table I shows a significant reduction in the numbers of metal atoms that are not nearest neighbors to any polymer interaction site. The algorithm used to simulate the initial flash evaporated surface yields a number of small metal atom clusters that result from the deposition of metal atoms on top of each other. The distribution of these clusters is determined by the statistics associated with randomly distributing one-quarter of a monolayer of metal atoms over the lateral dimensions of the film. Turning the interaction off between metal atoms during the anneal enables many of the metal atoms that are not bound to any of the interaction sites to migrate into the vacuum and eventually be lost to the system. One expects a smaller number to become bound to the polymer interaction sites. Note that the total loss of metal atoms during approach to steady state approximates the loss of metal atoms that are not bound to any interaction site, whereas the increase in metal atoms bound to two interaction sites approximates the loss of metal atoms bound to a single interaction site.

It should be further noted from the table that there is only one metal atom bound simultaneously to three or more interaction sites. This occurrence is rare since such a cluster would involve significant repulsion between interaction sites that are next nearest neighbors to each other. Furthermore, most of the clusters consisting of a single metal atom bound to two interaction sites form a linear complex, i.e., consist of interaction sites on opposite sides of the metal atom. This is a simple consequence of the magnitude of the repulsive energy chosen between next-nearest-neighbor interaction sites. There are no metal atoms bound to four or more polymer interaction sites.

We can perform a crude check to see if the simulated diffusion into the film is what would be expected from the choice of model parameters. For simple Fickian diffusion one expects the mean-squared displacement per metal atom in the film to be given by, approximately, $2Dt$, during time t. We have found close correspondence between this simple estimate with that calculated from the simulation. Calculating the root-mean-squared displacement into the film for 25 s of simulated diffusion yields a value of approximately 15 lattice spacings.

b. Nonvanishing Metal Atom Interaction. Next we discuss the results of the simulation in the presence of a nonvanishing metal atom interaction. The original motivation for these studies was provided by transmission electron microscopy of the copper–polyimide interface.[6] It was found that the annealing of several monolayers of copper deposited onto a clean PMDA–ODA polyimide surface resulted in copper migration into the polymer with the formation of copper globules that were roughly spherical in shape. To reproduce the shape of such globules with the original 2-D Monte Carlo simulations, nearest-neighbor and next-nearest-neighbor metal interactions were chosen to be strong and of equal strength. This was essential for the formation of the circular-like shapes of the globules obtained.[6] Sander has previously discussed a criterion for the formation of either "nonfractal" globular objects or ramified fractal objects.[12] The criterion involves the relative stability of the radial and angular deformations of a spherical cluster. For the metal atom clusters of the present simulation, this relative stability is determined by the strength and range of the metal atom interaction energies.

Table II

clusters	trial 1	trial 2	clusters	trial 1	trial 2
total	844	843	7	3	9
1	423	412	8	2	2
2	225	239	9	3	0
3	109	93	10	3	0
4	48	58	11	0	1
5	20	25	12	1	0
6	7	4			

To illustrate this we have treated two different cases: One for which the metal atom next-nearest-neighbor interaction energy is equal to the nearest-neighbor interaction energy and one for which the next-nearest-neighbor interaction energy is zero. These will be referred to as the strong and weak interactions, respectively.

Furthermore, two simulations have been performed for each set of different interaction energy values. This has been done to yield a crude check on the statistical significance of the results. We have, therefore, traced the thermodynamic relaxation of two ensemble members for each different set of metal atom interaction parameters. The relatively long cpu times required for each simulation preclude the possibility of making a more detailed check on the statistics.

All nonvanishing interaction energies chosen are large compared with the 320 °C thermal energy at anneal; i.e., the metal atom interaction energies are 1.0 eV compared with the annealing energy of about 0.05 eV. Therefore, in a manner similar to most of the diffusion limited aggregation (DLA) studies,[13] the metal atoms will bind strongly when they encounter each other, with, however, a small but not insignificant probability of subsequently breaking apart.

The initial interface resulting from the deposition conditions previously described can be thought of as arising from a "ballistic deposition" process.[14] Table II lists results obtained by simulating the flash evaporation for two independent trials. A cluster analysis has been performed for this initial "evaporation". While the definition of a cluster is arbitrary, we will, in all results to be presented (except those of Figure 3b), assume that any two metal atoms that are either nearest neighbors or next nearest neighbors to each other belong to the same cluster. Quantities of physical interest will determine the appropriate definition of a cluster with respect to any specific experiment or measurement. The present definition of a cluster that we have adopted would be appropriate if we were interested in treating cluster agglomeration and diffusion resulting from the cooperative motion of two or more strongly interacting metal atoms. Table II lists the total number of clusters as well as a breakdown into clusters containing a single metal atom, two metal atoms, three metal atoms, and so forth. One sees that the two independent trials yield differences in cluster number that are generally less that 20%. Also, there are more clusters containing a single metal atom than those with two or

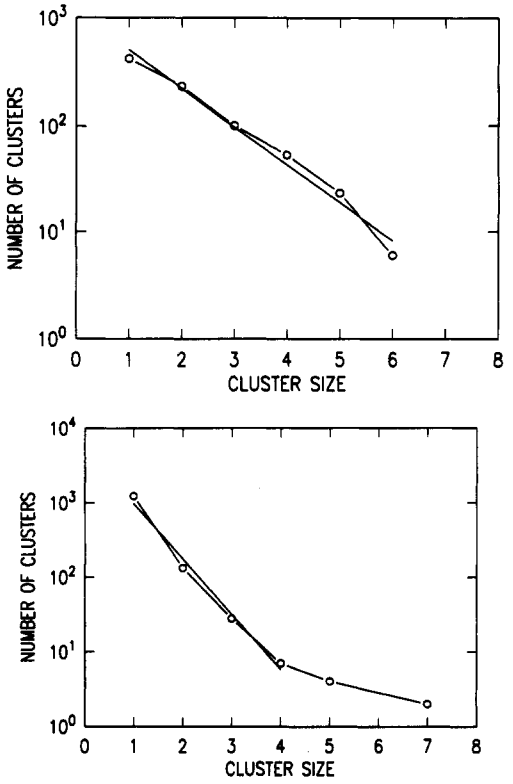

Figure 3. Semilog plot of cluster number as a function of cluster size for the initial "flash deposited" distribution. (a, Top) Nearest- and next-nearest-neighbor metal atoms defined as belonging to a cluster. (b, Bottom) Only nearest-neighbor metal atoms defined as belonging to a cluster.

more metal atoms. Decreasing numbers of clusters consisting of two, three, four, etc. metal atoms are found.

Figure 3a shows a semilog plot of cluster number, N, as a function of cluster size, S, for this initial distribution. We have taken the arithmetic average of the two different trials for the initial deposition to generate this figure. Note that, over the small cluster size ranging from one to six atoms, the distribution follows the relationship $N = N_0 \exp(-\eta S)$, as discussed by Meakin and Deutsch.[15] Least-squares fitting the result over this range of cluster size yields $\eta = -0.83 \pm 0.058$.

Figure 3b shows a plot similar to that of Figure 3a, except that we have now defined a cluster to include metal atoms coupled only at nearest-neighbor grid positions. Cluster number now falls off more rapidly with cluster size than in Figure 3a and exhibits a greater deviation from exponential behavior. Over the limited range of small cluster size shown, least-square fitting to an exponential decay yields a value of $\eta = -1.70 \pm 0.14$.

Figure 4 shows the number of nearest-neighbor polymer interaction sites bound to each of the metal atoms as the anneal progresses. The "time interval" is given in number of Monte Carlo cycles at the top of the figure. Results are shown for a simulation involving the strong metal atom interaction, Figure 4a, and for a simulation involving the weak interaction, Figure 4b. Identical initial distributions of metal atoms and interaction sites have been used in the two different simulations. One sees that initially there are few metal atoms that are bound to two interaction sites; however, as time progresses this number increases. The inset in the figures shows the first six data points on an expanded scale.

For the more weakly bound metal atom system, Figure 4b, one notes, upon anneal, a more rapid initial jump in the numbers of "free" metal atoms as well as a more rapid

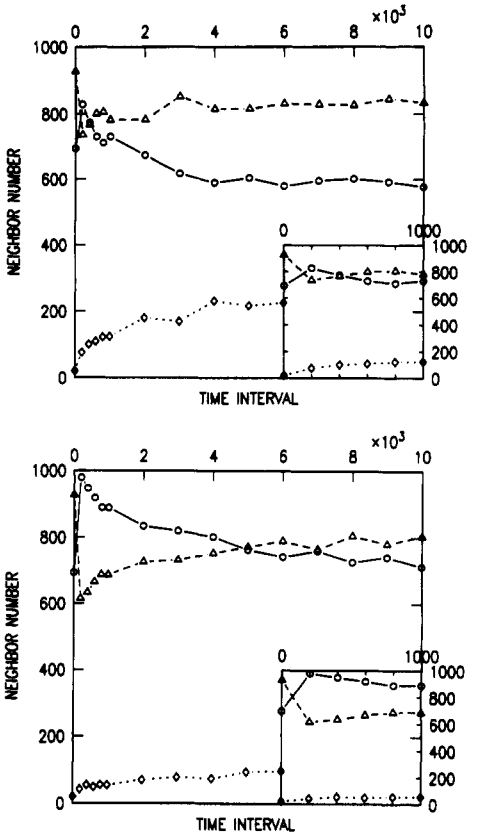

Figure 4. Number of polymer interaction sites that are neighboring the metal atoms: open circles, number of free metal atoms—no neighboring polymer interaction sites; open triangles, number of metal atoms bound to one polymer interaction site; open diamonds, number of metal atoms bound to two interaction sites. (a, Top) Strong interaction: next-nearest-neighbor interaction turned on. (b, Bottom) Weak interaction: next-nearest-neighbor interaction turned off.

decrease in the number of metal atoms bound to a single site. The system with the stronger metal atom interaction is also seen to exhibit a more rapid evolution to a quasi steady state. As a check on the long time evolution of both systems, i.e., the approach to quasi steady state, the calculations have been run for a period of time greater by an order of magnitude than the time interval displayed in the figures. Quasi-steady-state results have been obtained for 120 000 Monte Carlo iterations or approximately 10 min of annealing time for the strongly interacting system and 170000 Monte Carlo cycles or about 14 min of annealing time for the weakly interacting system.

Further comparison of parts a and b of Figure 4 shows that as time progresses the number of metal atoms bound to a single host interaction site approaches comparable values. Figure 4b shows the increase in number of metal atoms bound to two interaction sites to be somewhat less rapid than shown in Figure 4a. The former figure shows a slow growth of this number with time, and we have found that at times considerably longer than displayed in the figure, the number of weakly interacting metal atoms bound to two interaction sites is approximately 15% less than that achieved with the more strongly interacting system. One therefore concludes that over the long term, the numbers of polymer interaction sites bound to each of the metal atoms is not significantly affected by the different choice of metal atom interaction strength.

Figure 5a shows a slice of the film that is perpendicular to one of the lateral dimensions. The distribution of interaction sites and metal atoms is shown at steady state for the strong metal atom interaction simulation. One

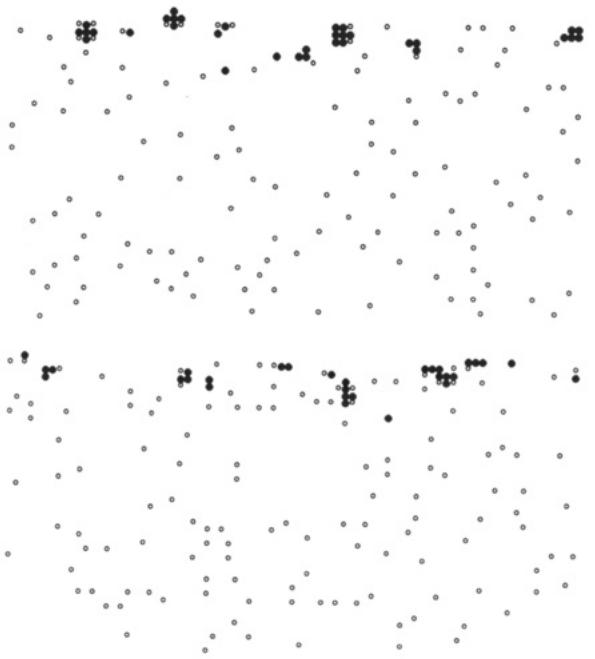

Figure 5. Distribution of metal atoms and interaction sites in one particular slice of the film that is perpendicular to one of the lateral directions: filled circles, metal atoms; open circles, polymer interaction sites. (a, Top) Strong interaction: next-nearest-neighbor interaction turned on. (b, Bottom) Weak interaction: next-nearest-neighbor interaction turned off.

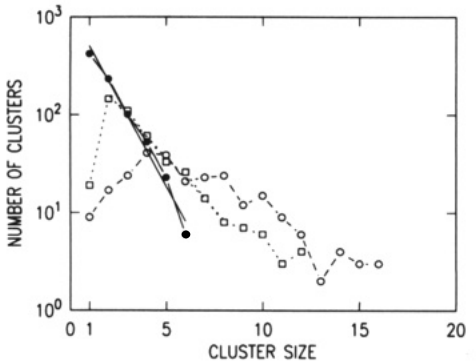

Figure 6. Semilog plot of cluster number as a function of cluster size: filled circles, initial metallization; open squares, quasi steady state—weak metal interaction; open circles, quasi steady state—strong metal interaction.

sees, for this particular slice, several clusters composed of metal atoms bound to two interaction sites. Figure 5b shows a similar slice obtained, however, for the weak interaction. As in the previous figure we have selected a slice that illustrates the binding of two interaction sites to a metal atom. Also, consistent with a previous observation, one sees no pair of interaction sites in this plane that are nearest neighbors to the same metal atom and next nearest neighbors to each other. It should be noted that even though we are examining just a plane through clusters composed of a relatively small number of metal atoms, the effect of different interaction strength on cluster shape is apparent.

Figure 3a displays cluster number as a function of cluster size for the simulated initial evaporated distribution of copper atoms. In Figure 6 we overlay the results for the strongly interacting as well as weakly interacting copper simulations at steady state. Data used in generating the figure have been obtained by averaging the results of the two independent trials. Upon annealing, one sees a dramatic decrease in the number of single metal atom clusters. The weakly interacting model yields exponential behavior, however, over only a range of cluster size from two to eight atoms. Fitting the exponential relationship discussed by Meakin and Deutch[15] over this range yields a value of $\eta = -0.48 \pm 0.02$. Data for the strongly interacting model are more widely scattered, with the cluster size peaking at a value equal to four metal atoms.

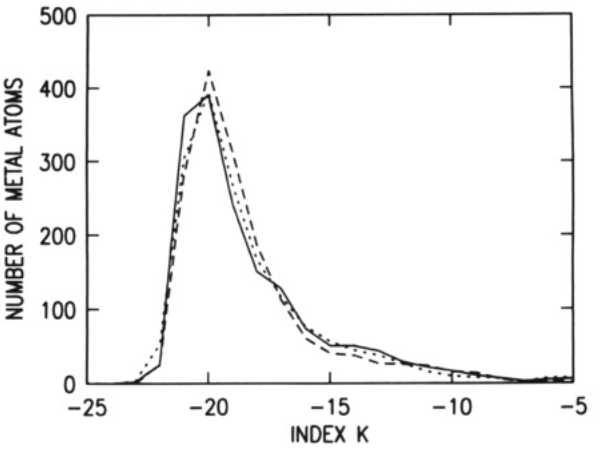

Figure 7. Number of metal atoms at different depths into the film: solid line, initial metallization; dotted line, weak metal interaction; dashed line, strong metal interaction.

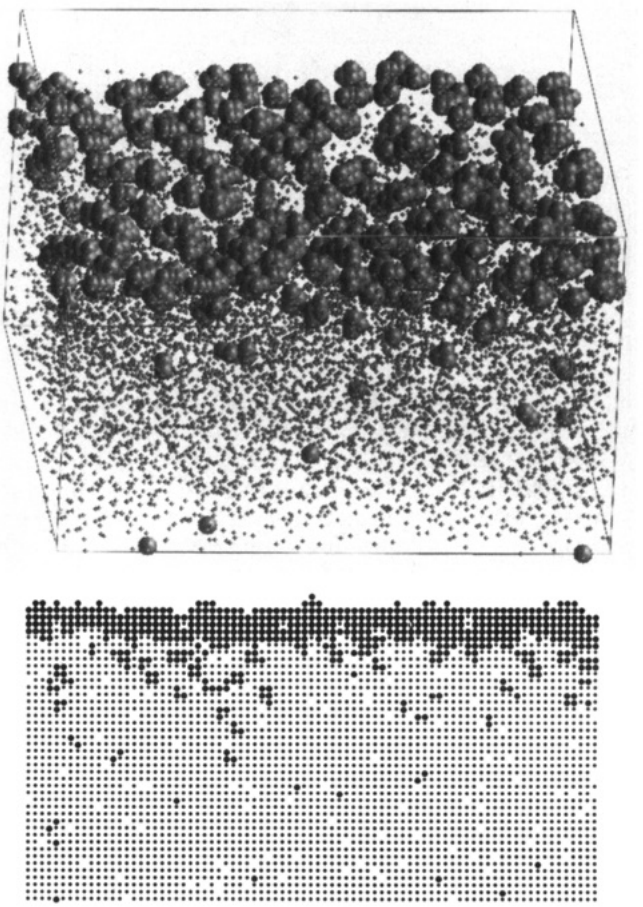

Figure 8. (a, Top) Three-dimensional view, at an angle to the top film surface, at quasi steady state for the strongly interacting system. The metal atoms are shown as larger spheres. (b, Bottom) Metal atom penetration profile into the film at quasi steady state for the strongly interacting system.

Figure 7 shows the number of metal atoms at different depths into the film, i.e., as a function of the index k. We have averaged the results for the two independent trials.

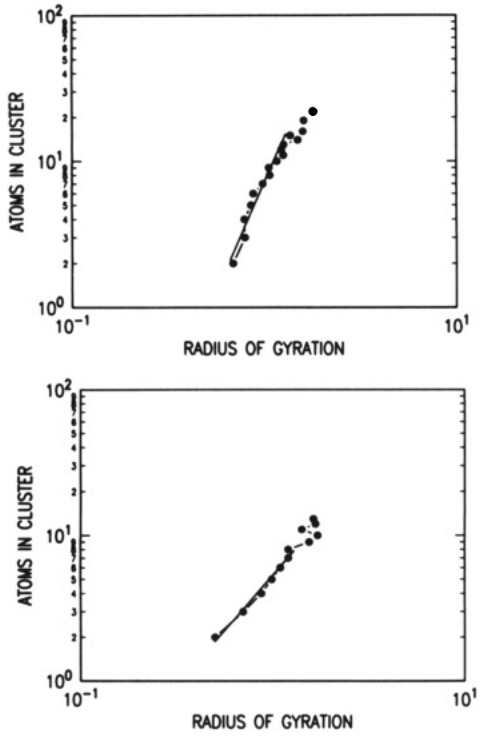

Figure 9. log–log plot of cluster size as function of radius of gyration: (a, top) strong metal atom interaction; (b, bottom) weak metal atom interaction.

One sees that over the time it takes to achieve quasi steady state there is little net atom migration into the film. The three curves in the figure are not far from being superimposed. Examination of the figure does, however, reveal a small but systematic shift of the metal atom distribution into the film upon annealing. Most of the metal atoms cluster at or near the surface of the film with several single metal atoms migrating into the bulk. The small number of additional metal atoms that have migrated above the surface of the film for the more weakly interacting simulation should also be noted.

Figure 8a shows a three-dimensional view at an angle to the top surface after steady state has been achieved for the strongly interacting metal atom simulation. This should be compared with Figure 2a, the 3-D metal atom distribution prior to annealing. Figure 8b is an edge-on view of the film for the same distribution illustrated in Figure 8a. This figure displays the metal atom penetration into the film and has been generated in a manner similar to Figure 2b. Comparison of Figure 8b with Figure 2b provides a visual measure of metal atom penetration into the film upon annealing. A rough estimate of the ratio of the density of metal atoms closely clustered at the surface to the density of the single metal atoms that have migrated into the bulk is qualitatively in accord with the relative densities obtained from the tracer diffusion studies.[7]

Finally, we say a few words about the effect of metal atom interaction strength on the shape of the clusters and consequently upon the calculated fractal dimensionality. Figure 9 is a plot of the cluster size or number of atoms in the cluster, S, as a function of the radius of gyration, R_g. The radius of gyration has been obtained as an average over clusters of the same size. The fractal dimension, D, of the clusters has been found from $S = AR_g^D$. For the strong metal interaction, Figure 9a, the fractal dimensionality is found to be 2.98 ± 0.31, which reflects the globular nature of the clusters. The weak interaction, Figure 9b, on the other hand, yields clusters with a fractal

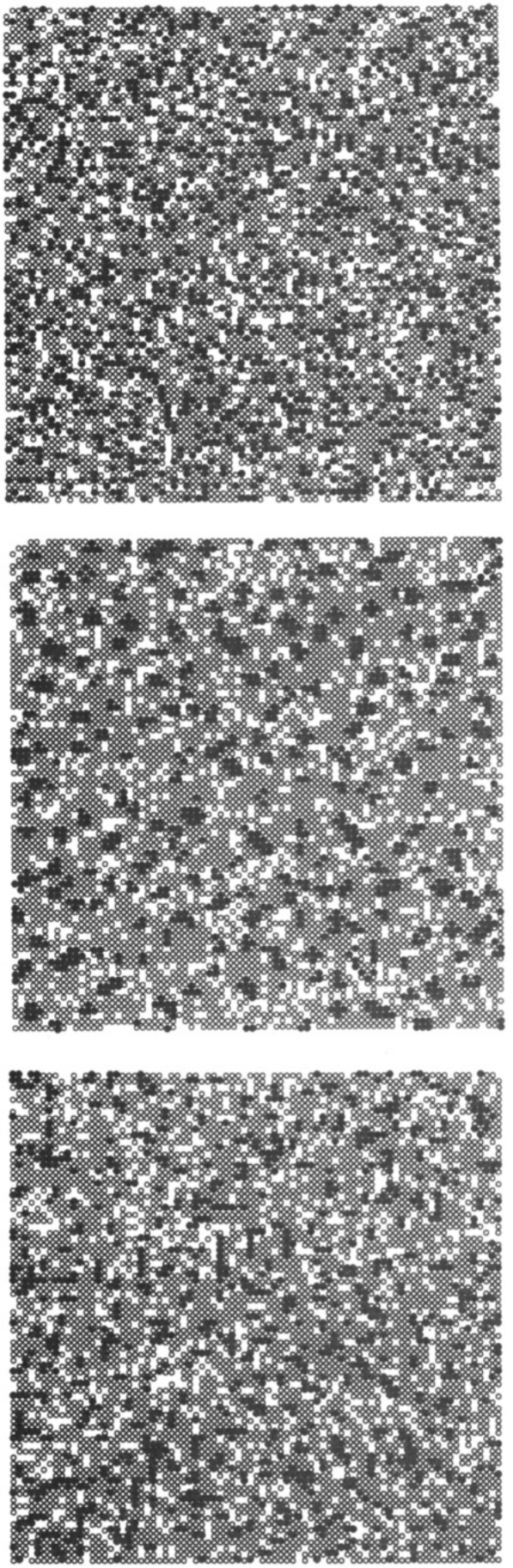

Figure 10. Top view of the film surface: (a, top) after initial "flash evaporation"; (b, middle) quasi steady state of the strongly interacting system; (c, bottom) quasi steady state of the weakly interacting system.

dimension of 1.50 ± 0.10, reflecting the more elongated structure of the clusters. As previously mentioned, one can consider the difference between the behavior exhibited by the strong and weak metal atom interactions to be a consequence of differences in the relative stability of the angular and radial deformations induced in a spherical-like cluster.[12]

Figure 10 shows a top view of the metal-deposited surfaces, initially and at quasi steady state for the two interaction models. In generating the figure it has been assumed that one sees only the uppermost occupied species along the line of sight. The difference between this procedure and that used to generate Figures 2b and 8b should be noted. An empty grid position indicates that along the line of sight there is neither a metal atom nor polymer interaction site through the entire film thickness. Even for the relatively small number of metal atoms displayed, one can clearly discern the more compact structure of the metal atom clusters for the more strongly interacting case. It is apparent that the stronger metal atom interaction will yield more compact clusters of higher fracal dimensionality.[16]

Perhaps it should be emphasized that since we are dealing with clusters composed of relatively few metal atoms, the discrete nature of the three-dimensional simple cubic lattice imposes a significant constraint on the calculated radii of gyration and consequently on the calculated fractal dimensionality. Furthermore, the observation of only incipient ramification compared with that obtained for much of the diffusion-limited aggregation (DLA) literature[13] is one more consequence of the small number of metal atoms in the present simulation; a feature dictated by the radiotracer diffusion studies that we have attempted to simulate.

IV. Conclusions

The present simulations have attempted to provide insight into the role played by metal atom interactions during formation of a metal–polyimide interface. Such interactions have been shown to determine the details of cluster formation during the incipient stage of interface formation as well as to inhibit metal atom diffusion into the film and reemission into the vacuum. These interactions, together with the interactions between metal and polymer, are responsible for determining the detailed properties of the metal–polymer interface. The interface model that we have investigated lends itself to many further inquiries. Variations in temperature, free volume, metal atom deposition rate, and metal atom–polymer interaction strength will affect the metal polymer interface and are several of the factors that would be worthwhile examining in future simulations.

Acknowledgment. I thank Dan Platt for several valuable discussions concerning diffusion-limited aggregation (DLA) and Cliff Pickover for assistance with the three-dimensional graphics.

References and Notes

(1) Polyimides: Materials, Chemistry and Characterization. *3rd Ellenville Conference Proceedings*; Feger, C., Khojasteh, M. M., McGrath, J. E., Eds.; Elsevier: Amsterdam, 1989.
(2) Shanker, K.; MacDonald, J. R. *J. Vac. Sci. Technol.* **1987**, *5*, 2894.
(3) Kim, Y.-H.; Walker, G. F.; Kim, J.; Park, J. *J. Adhesion Sci. Technol.* **1987**, *1*, 331.
(4) Currie, J.; Depelsenaire, P.; Groleau, R.; Sacher, E. *J. Colloid Interface Sci.* **1984**, *97*, 410.
(5) Jensen, R. J.; Cummings, P.; Vora, H. *IEEE Transactions on Components, Hybrids, and Manufacturing Technology*; CHMT-7, 1984; p 384.
(6) LeGoues, F. K.; Silverman, B. D.; Ho, P. S. *J. Vac. Sci. Technol.* **1988**, *A6*, 2200.
(7) Faupel, F.; Gupta, D.; Silverman, B. D. *Appl. Phys. Lett.* **1989**, *55*, 357.
(8) Muller-Krumbhaar, H. In *Monte Carlo Methods in Statistical Physics*; Binder, K., Ed.; Springer Verlag: Berlin, 1979; pp 261.
(9) Frisch, H. L.; Stern, S. A. *CRC Rev. Solid State Mater. Sci.* **1983**, *11*, 123.
(10) Metropolis, N.; Rosenbluth, A. W.; Rosenbluth, M. N.; Teller, A. H.; Teller, E. *J. Chem. Phys.* **1953**, *21*, 1087.
(11) Binder, K.; Stauffer, D. In *Applications of the Monte Carlo Method in Statistical Physics*; Ed. Binder, K., Ed.; Springer Verlag: Berlin, 1984; p 7.
(12) Sander, L. M. In *Kinetics of Aggregation and Gelation*; Family, F.; Landau, D. P., Eds.; Elsevier Science Publishers B. V.: Amsterdam, 1984; p 13.
(13) The following is a partial list of books concerned with diffusion-limited aggregation (DLA) and useful within the context of the present discussion: *Kinetics of Aggregation and Gelation*; Family, F., Landau, D. P., Eds.; North-Holland: Amsterdam, 1984. *The Fractal Approach to Heterogeneous Chemistry*; Avnir, D., Ed.; John Wiley and Sons: New York, 1989. *Random Fluctuations and Pattern Growth: Experiments and Models*, Stanley, H. E., Ostrowsky, N., Eds.; Kluwer Academic Publishers: Dordrecht, 1988. *Scaling Phenomena in Disordered Systems*; Pynn, R., Skjeltorp, A., Eds.; Plenum Press: New York, 1985. Feder, J. *Fractals*; Plenum Press: New York, 1988. *On Growth and Form*; Stanley, H. E., Ostrowsky, N., Eds.; Martinus Nijhoff Publishers: Dordrecht, 1986.
(14) Meakin, P.; Ramanlal, P.; Sander, L. M.; Ball, R. C. *Phys. Rev. A* **1986**, *34*, 5091.
(15) Meakin, P.; Deutsch, J. M. *J. Chem. Phys.* **1985**, *83*, 4086.
(16) Private communication. Platt and Family have considered a model with nearest and next nearest neighbors sticking in DLA. They observed that the change in this interaction from only a nearest-neighbor interaction changed the lower cutoff of the scaling regime and changed the mass–radius scaling by a multiplicative factor without affecting the scaling exponent. This was consistent with other results indicating that physical properties such as surface tension also primarily changed the lower cutoff in the scaling regime but did not change the scaling exponent. For the present situation, the cluster sizes are all near or at the length scale of the interaction and are, therefore, on the edge of the scaling regime of a DLA-type calculation. The fractal character of the DLA growth patterns is determined by the topological shielding (screening) of the ramified growing structure, which requires that the cluster bonds last much longer than the diffusive growth process itself. In a more near-equilibrium situation, such shielding is reduced, and the clusters lose their fractal character.

Registry No. (PMDA)(ODA) (copolymer), 25038-81-7; (PMDA)(ODA) (SRU), 25036-53-7; Ca, 7440-50-8.